REFERENCES

1. Chu T, D'Angio GJ, Favara B, Ladisch S, Nesbit M, Pritchard J. Histiocytosis syndromes in children. *Lancet* 1987;1:208–209.
2. Resnick D. Lipidoses, Histiocytoses and hyperlipoproteinemias. In: *Diagnosis of bone and joint disorders, 2nd ed.* Philadelphia: W.B. Saunders; 1988:2404–2459.
3. Gilday DL, Ash JM, Reilly BJ. Radionuclide skeletal survey for pediatric neoplasms. *Radiology* 1977;123:399–406.
4. Hanley JA, McNeil BJ. The meaning and use of the area under a receiver operating characteristic (ROC) curve. *Radiology* 1982;143:29–36.
5. Hanley JA, McNeil BJ. A method of comparing the areas under receiver operating characteristic curves derived from the same cases. *Radiology* 1983;148:839–843.
6. The International Commission of Radiological Protection. ICRP Publication 34, Protection of the patient in diagnostic radiology. Oxford, England: Pergamon Press; 1982:53–77.
7. Weber DA, Makler PT, Watson EE, Coffey JL. Radiation absorbed dose from ^{99m}Tc-labeled bone imaging agents. *J Nucl Med* 1989;30:1117–1122.
8. Kereiakis J, Rosenstein M, Bocaraton F. Handbook of radiation doses in nuclear medicine and diagnostic x-ray. Colorado: CRC Press; 1980:165.
9. Berry DH, Becton DL. Natural history of Histiocytosis X. Haem/Oncol Clin N Am 1987;1:23–35.
10. Favara BE, McCarthy RC, Mierau GW. Histiocytosis X. Hum Pathol 1983;14:663–676.
11. Avery ME, McAfee JG, Guild HG. The course and prognosis of reticuloendotheliosis (eosinophilic granuloma, Schuller-Christian disease and Letterer-Siwe disease). A study of forty cases. *Am J Med* 1957;22:636–652.
12. Gianotti F, Caputo R. Histiocytic syndromes: a review. *J Am Acad Dermatol* 1985;13:383–404.
13. Ceci A, De Terlizzi M, Colella R, et al. Langerhans cell histiocytosis in children: results from the Italian co-operative AIEOP-CNR-H.X'83 study. *Med Pediatr Oncol* 1993;21:259–264.
14. Enriquez P, Dahlin DC, Hayles AB, Henderson ED. Histiocytosis X: a clinical study. *Mayo Clin Proc* 1967;42:88–99.
15. Sims DG. Histiocytosis X. Follow-up of 43 cases. *Arch Dis Child* 1977;52:433–440.
16. Cline MJ, Golde DW. A review and re-evaluation of the histiocytic disorders. *Am J Med* 1973;55:49–60.
17. Sartoris DJ, Parker BR. Histiocytosis X: rate and pattern of resolution of osseous lesions. *Radiology* 1984;152:679–684.
18. Martinez-Lage J, Poza M, Cartagena J, Vincente J, Biec F, De Las Heras M. Solitary eosinophilic granuloma of the pediatric skull and spine. *Childs' Nerv Syst* 1991;7:448–451.
19. Schaub T, Ash JM, Gilday DL. Radionuclide imaging in histiocytosis X. *Pediatr Radiol* 1987;17:397–404.
20. Parker BR, Pinckney L, Etcubanas E. Relative efficacy of radiographic and radionuclide bone surveys in the detection of the skeletal lesions of Histiocytosis X. *Radiology* 1980;134:377–380.
21. Antonmattei S, Tetalman MR, Lloyd TV. The multi-scan appearance of eosinophilic granuloma. *Clin Nucl Med* 1979;4:53–55.
22. Kumar R, Balachandran S. Relative roles of radionuclide scanning and radiographic imaging in eosinophilic granuloma. *Clin Nucl Med* 1980;5:538–542.
23. Siddiqui AR, Tashijan JH, Lazarus K, Wellman HN, Baehner RL. Nuclear medicine studies in evaluation of skeletal lesions in children with Histiocytosis X. *Radiology* 1981;140:787–789.
24. Westra SJ, VanWoerden H, Postma A, Elema JD, Piers DA. Radionuclide bone scintigraphy in patients with Histiocytosis X. *Eur J Nucl Med* 1983;8:303–306.
25. Fezoulidis I, Wickenhauser J, Schurawitzki H, Gritzmann N. Histiozytosis X: szintigraphische und rontgenologische Befunde. *Rontgen-Bl* 1987;40:234–239.
26. Crone-Munzebrock W, Brassow F. A comparison of radiographic and bone scan findings in Histiocytosis X. *Skeletal Radiol* 1983;9:170–173.
27. George JC, Buckwalter KA, Cohen MD, Edwards MK, Smith RR. Langerhans cell histiocytosis of bone: MR imaging. *Pediatr Radiol* 1994;24:29–32.

Radionuclide Venography and Its Functional Analysis in Superior Vena Cava Syndrome

Asif Mujtaba Mahmud, Toyoharu Isawa, Takeo Teshima, Tomio Hirano, Yoshiki Anazawa, Makoto Miki and Toshihiro Nukiwa

Department of Respiratory Medicine, Institute of Development, Aging and Cancer (formerly Research Institute for Chest Diseases and Cancer), Tohoku University, Sendai, Japan

In addition to imaging, radionuclide venography maybe used for the functional assessment of superior vena cava (SVC) syndrome by applying the indices of transit time (TT), time of half-peak count (TH) and peak count ratio (PC ratio). **Methods:** Ten healthy subjects (Group N) and 107 patients with SVC syndrome (64 symptomatic and 43 asymptomatic) were studied. Images were visually assessed for collaterals or jugular venous reflux and values of the indices were calculated. **Results:** The 107 patients were subclassified into three groups according to the images obtained. Collateral circulation was seen in 37 patients (Group C). In 20 patients, jugular venous reflux was observed (Group J). Fifty patients who showed neither collaterals nor reflux were included in Group P. In comparison to Group N [3.6 ± 0.56 sec (sem)], TT values were significantly higher ($p < 0.05$) for Group J (7.13 ± 1.16 sec) and Group C (7.00 ± 0.87 sec). Values of TH were significantly prolonged ($p < 0.05$) for Group J (23.6 ± 4.8 sec) and Group C (18.8 ± 2.2 sec) in comparison to Group N (9.2 ± 1.5 sec). PC ratio values were higher in all patient groups in comparison to Group N (3.4 ± 0.57). **Conclusion:** These indices are potentially useful in the initial diagnosis and post-therapeutic evaluation of SVC syndrome. In the absence of other causes, appearance of jugular venous reflux may be considered a sign of SVC syndrome.

Key Words: radionuclide venography; superior vena cava syndrome; jugular venous reflux; functional indices

J Nucl Med 1996; 37:1460–1464

Superior vena cava (SVC) syndrome was first described by William Hunter in 1757 (*1*). Presently, bronchogenic carcinoma is the leading cause and accounts for 67%–82% of all cases of SVC obstruction (*2*). Initially, SVC syndrome was considered to be an oncologic emergency (*3*), but later reports have refuted this notion (*4–6*). Emergency or not, it bears considerable importance for both the clinician and patient.

A careful diagnostic work-up is an essential prerequisite to successful management of this syndrome (*4,6*). Radionuclide venography is a convenient, noninvasive procedure which forms an important component of such a work-up (*2*). In the present study, we intended to establish certain criteria on radionuclide venography to aid in the diagnosis and post-therapeutic evaluation of SVC syndrome and to study hemodynamic characteristics in the central veins, consequent to stenosis and/or obstruction of the SVC.

METHODS

Subjects

Between February 1986 and July 1994, radionuclide venography was performed on 117 subjects. Ten healthy volunteer men (aged 31–57 yr; mean age 43 yr) constituted the control Group N. The remaining 107 were patients with SVC syndrome (97 men, 10 women; age 33–81 yr; mean age 62.6 yr). Selection criteria included presence of clinically obvious SVC syndrome consisting of swelling of the face, neck and/or the upper extremities (symptomatic in 64 patients) or only radiological signs such as mediastinal widening, suprahilar or hilar lesions and tumor location in upper lung zones, rendering them susceptible to SVC syndrome-

Received May 30, 1995; revision accepted Nov. 3, 1995.

For correspondence or reprints contact: Asif Mujtaba Mahmud, Department of Respiratory Medicine, Institute of Development, Aging and Cancer, Tohoku University, 4-1 Seiryoumachi, Aoba-ku, Sendai 980, Japan.

(asymptomatic in 43 patients). More than three of four had bronchogenic carcinoma. The diagnostic profile is shown in Table 1.

Data Acquisition

Boluses of 111 MBq (3 mCi) ^{99m}Tc-MAA, less than 0.5 ml in volume, were injected simultaneously into both median cubital veins of the subjects lying in the supine position with their arms by their sides and holding the neck in the neutral position, i.e., the back and occiput touching the examination table. They were asked to continue normal tidal breathing, avoiding Valsalva's maneuver (*7*). The gamma camera was placed anteriorly over the neck and the upper chest. Data were stored in frame mode at 1 frame/sec for 2 min at 64 × 64 matrices. This was followed by lung perfusion imaging in anterior, posterior, right and left lateral views in sitting position.

Data Analysis

Images were carefully assessed visually for the presence of collaterals or internal jugular venous reflux. The stored data then were processed by a computer as follows. After image addition, four regions of interest (ROIs), depending on the anatomical size of the vessel, were drawn with one each on the right and left subclavian veins (RSCV and LSCV) (6 × 10 matrix size), the superior vena cava (SVC) (4 × 12 matrix size) and the right atrium (RA) (6 × 9 matrix size) (Fig. 1). The size of each ROI corresponds to the normal dimensions of the respective vessel. A time-activity curve was plotted for each ROI (Fig. 1). The curves for the subclavian veins showed single peaks. On the other hand, two peaks were usually visible on the curves for the SVC and the RA corresponding to the entry of radionuclide from the RSCV and the LSCV. The points on the curves were denoted as PC = peak count, PT = peak time, PC/2 = half-peak count and TH = time of half-peak count. The subscript RSCV, LSCV or SVC denotes the vessel from which the curve was derived. R and L denote peaks produced by the bolus from the right and left subclavian veins. The first peak is marked R because peak time in the RSCV was earlier, as compared with the peak time in the LSCV, in the majority of cases. In patients with earlier peaks on the left side, the first peak was accordingly considered to be caused by the left subclavian bolus. Appearance of a single peak indicated concurrent entry of boluses from the subclavian veins.

$PT_{RA(R)}$ = peak time in the right atrium, produced by the bolus from RSCV

$PT_{RA(L)}$ = peak time in the right atrium, produced by the bolus from LSCV.

As explained earlier, the converse was considered in patients with earlier left subclavian vein peaks. The following three indices were defined and their values were calculated for each subject, according to:

Transit time is:

$$TT(R) = PT_{RA(R)} - PT_{RSCV}$$

$$TT(L) = PT_{RA(L)} - PT_{LSCV},$$

where TT(R) denotes transit time of the bolus from the RSCV to the RA and is calculated by subtracting the peak time in the RSCV from the time of the peak produced in the RA by the right subclavian bolus. Similarly, TT(L) means transit time from the LSCV to the RA and is calculated by using corresponding values on the left side.

Time of half-peak count is:

$$TH_{RSCV}$$

$$TH_{LSCV},$$

where TH is the time of half-peak count in the subclavian veins and is the time difference between the points of half PC on the curve (Fig. 1).

Peak count ratio is:

$$\text{PC ratio} = \text{Max}\{PC_{RSCV}, PC_{LSCV}\}/PC_{SVC}.$$

Peak count ratio was calculated by dividing the PC in the RSCV or LSCV, whichever was greater, by the PC in the SVC.

Statistical significance was determined with Bonferoni's multiple-comparison procedure (*8*), paired or unpaired t-test; a p value less than 0.05 was considered statistically significant.

RESULTS

Visual Assessment and Grouping

In Group N, no jugular venous reflux or collaterals were seen in the venograms of the 10 normal subjects (Fig. 2A). In Group P, 50 patients (46%) who showed neither collaterals nor jugular reflux were included (Fig. 2B).

Twenty patients (19%) showing only jugular venous reflux were classified as Group J (Fig. 2C). Of these, 11 had no clinical signs of SVC syndrome but had suggestive radiological signs. The remaining nine were symptomatic.

Thirty-seven patients (35%) showing various collaterals, as listed in Table 2, were categorized as Group C (Fig. 2D). In this group, seven patients showed no clinical manifestations of SVC syndrome. Certain common patterns of collaterals are shown in Figure 3.

Quantitative Analysis

Paired t-test analysis revealed no statistically significant difference between the TT(R) and TT(L) and the TH_{RSCV} and TH_{LSCV} in all four groups. Therefore, the higher of the two values was used for comparison since it was considered more indicative of the hemodynamic derangement. Since we depended on the appearance of clearcut upward and downward slopes on the time-activity curves of the subclavian veins and the appearance of two peaks on the curve for the RA, we could calculate TH or TT from one side only in a few cases having unclear curves. In addition, some cases with bizarre curves had to be omitted, which explains the discrepancy between the case number (n) presented on the graph and the total number for each group. In the case of the PC ratio, a single value was obtained from each subject.

Mean values of indices for each group were compared among the four groups (Bonferoni's method) and among the asymptomatic and symptomatic subgroups within each group (unpaired t-test). No statistical significance was seen in the latter case.

Transit Time

As shown in Figure 4, an upward trend of TT was observed, indicating that it is prolonged as the disease state progresses. No further prolongation was observed in Group C. In comparison to Group N (3.6 ± 0.56 sec), TT was significantly higher in Group J (7.13 ± 1.16 sec; $p < 0.05$) and Group C (7.00 ± 0.87 sec; $p < 0.05$). Group P differed significantly from Groups J ($p < 0.05$) and C ($p < 0.01$).

Time of Half-Peak Count

As illustrated in Figure 5, the TH in the subclavian veins was highest in Group J (23.6 ± 4.8 sec) which differed significantly

TABLE 1
Diagnostic Profile of Patients

Diagnosis	Number of patients
Bronchogenic carcinoma	(88)
Squamous-cell	26
Adenocarcinoma	25
Small-cell	22
Large-cell	15
Mediastinal tumors	13
Metastatic cancer	3
Miscellaneous	3
Total	107

from Groups N (9.2 ± 1.5 sec; $p < 0.05$) and P (13.2 ± 1.4 sec; $p < 0.05$).

Peak Count Ratio

The PC ratio showed an upward trend (Fig. 6) which was similar to the tendency observed for TT and TH. Although insignificant statistically, values were higher for all patient groups in comparison to Group N (3.4 ± 0.57). There was little difference between Group J (6.8 ± 2.55) and Group C (6.78 ± 0.97).

DISCUSSION

Radionuclide venography is a useful, accurate and noninvasive method of imaging the venous system (*9*). In addition to imaging, it can be used to study the functional aspects of SVC syndrome (*10*). Consistent with other large series, more than 80% of our patients had bronchogenic carcinoma, with squamous-cell carcinoma being the leading cell type (*2*). There were no patients with valvular heart disease, overt heart failure or thoracic venous catheters.

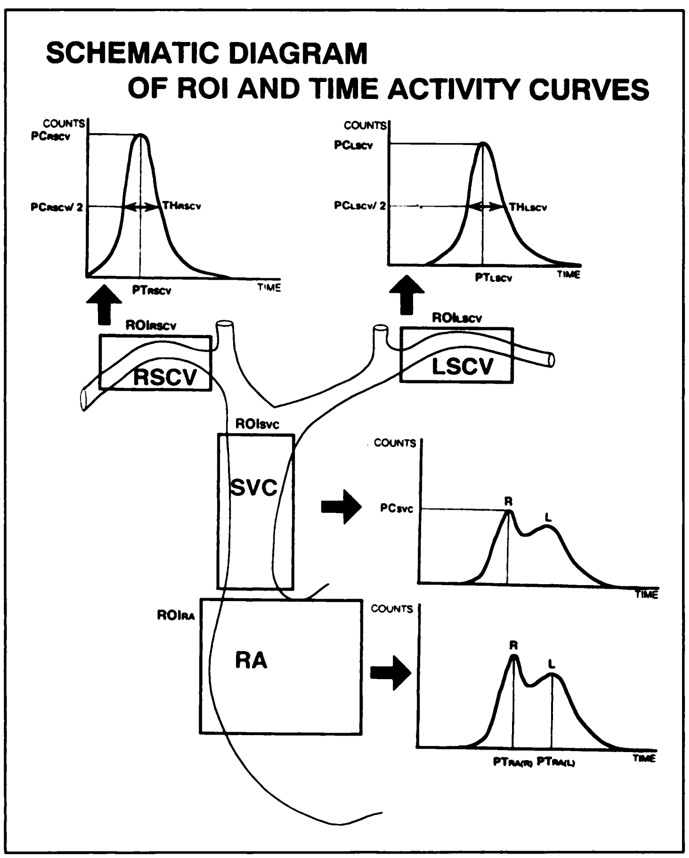

FIGURE 1. Diagram of four ROIs and relevant time-activity curves. PC = peak count; PT = peak time; TH = time of half-peak count; RSCV = right subclavian vein; LSCV = left subclavian vein; SVC = superior vena cava; RA = right atrium; $PT_{RA(R)}$ = peak time of bolus coming from right subclavian vein; $PT_{RA(L)}$ = peak time of bolus coming from left subclavian vein.

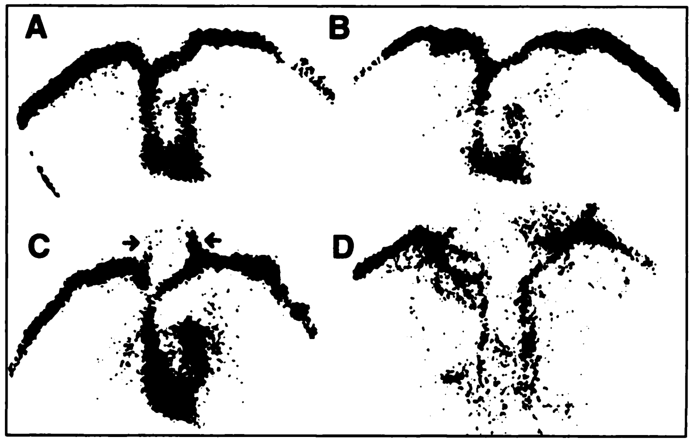

FIGURE 2. Venographic images of four subject groups. (A) Group N. (B) Group P. (C) Group J, note visualization of internal jugular veins bilaterally (arrows) indicating retrograde flow as a consequence of impaired flow through the SVC. (D) Group C, bilateral internal thoracic veins are seen as collaterals.

Collaterals

In our series, 37 patient (35%) showed collaterals, whereas Coltart et al. (*11*) encountered collaterals in 50%. The most common collateral pathways were the lateral thoracic, internal thoracic and intercostal veins. We used the term cervical venous network to denote the vertebral and highest intercostals as defined by Muramatsu (*12*). Twenty percent of the patients with collaterals were asymptomatic and, therefore, the presence of collaterals served as a confirmatory sign of SVC syndrome. Gradual development of the syndrome in cases with partial stenosis of the SVC may lead to such a phenomenon (*13*).

Jugular Venous Reflux

Jugular venous reflux has been observed by several authors in the course of dynamic brain flow imaging (*14–16*). Rao et al. (*16*) mentioned certain technical factors as possible causes of the reflux. Retrograde flow in the central veins of subjects with valveless cervical venous systems or cervical venous incompetence has also been implicated (*17*). It has also been described as a sign of elevated systemic venous pressure due to congestive heart failure (*18*). According to Peart and Driedger, appearance of jugular reflux warrants further investigation of the mediastinum (*19*). Miyamae encountered it, secondary to central vein obstruction, during radionuclide venography (*10*). Irrespective of the cause, retrograde flow seems to be the principal factor in the pathogenesis of the jugular reflux, even in cases with absent or incompetent cervical valves. In our series, reflux was

TABLE 2
Frequency of Collateral Pathways

Collateral	Number of patients
Lateral thoracic vein	15 (40.5%)
Internal thoracic vein	15 (40.5%)
Intercostal vein	15 (40.5%)
Jugular venous arch	10 (27%)
Cervical venous network	8 (21%)
External jugular vein	7 (19%)
Azygos vein	6 (16%)
Superior intercostal vein	4 (10%)

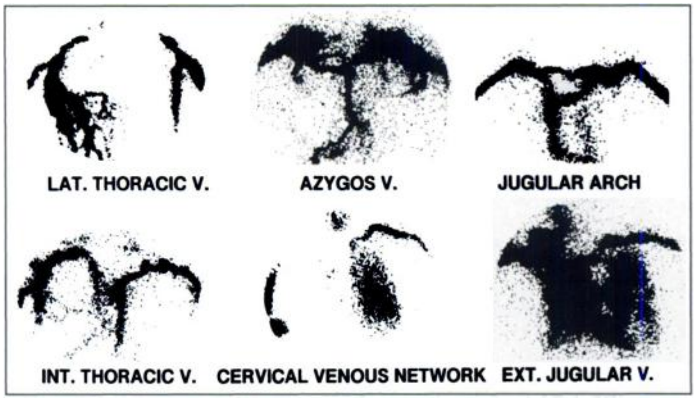

FIGURE 3. Frequent patterns of collateral circulation. Upper row from left to right: lateral thoracic vein, azygos vein, jugular arch. Lower row from left to right: internal thoracic vein, cervical venous network (*12*), external jugular vein.

associated with increased values of TT, TH and PC ratio in the presence of either clinical or only radiological signs of SVC syndrome. In addition, the absence of heart failure and avoidance of technical factors indicated SVC stenosis as the cause of retrograde flow leading to the appearance of jugular venous reflux. In Group J, 11 patients (>50%) did not have clinically overt SVC syndrome. The presence of jugular venous reflux in these patients could suggest the existence of SVC syndrome. It, therefore, served as a valuable and early sign of SVC obstruction.

Functional Indices

The appearance of two peaks in the curves from the SVC and the RA may be attributed to a slight discrepancy in timing of injections between the patient's two arms.

Transit time values for normal subjects (3.6 ± 0.56 sec) are concordant with those of Vincken et al. (*20*). We considered TT from the subclavian veins to the right atrium as most sensitive and specific for flow disturbance in the central veins, since it represents TT across our focus of interest (the central veins) and is independent of local factors, such as arm edema and position and axillary node swelling. Also, it is not influenced by the discrepancy in timing of injection. Other authors have calculated transit time of the bolus from the antecubital veins to the right heart (*10*) and its arrival time in the subclavian veins and the SVC from the arm (*9*). Local factors may exert an influence on these values. Figure 4 depicts an upward trend of TT among the four groups but no further prolongation is observed on opening of collateral pathways.

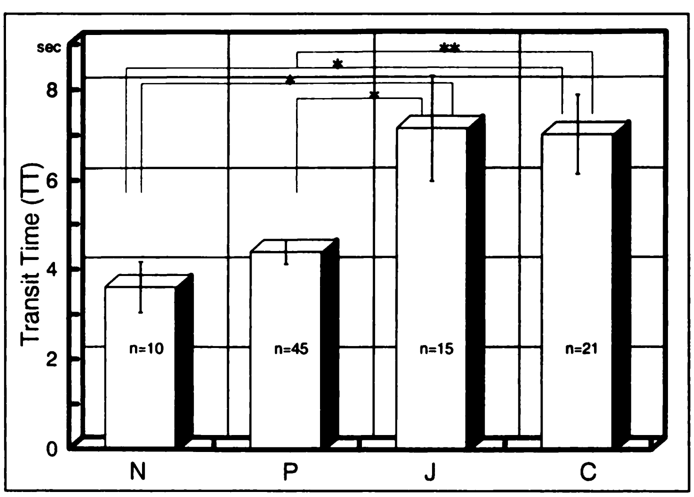

FIGURE 4. Comparison of transit time (TT) between normal subjects and patient groups. *: $p < 0.05$; **: $p < 0.01$. Error bars show 1 s.e.m.

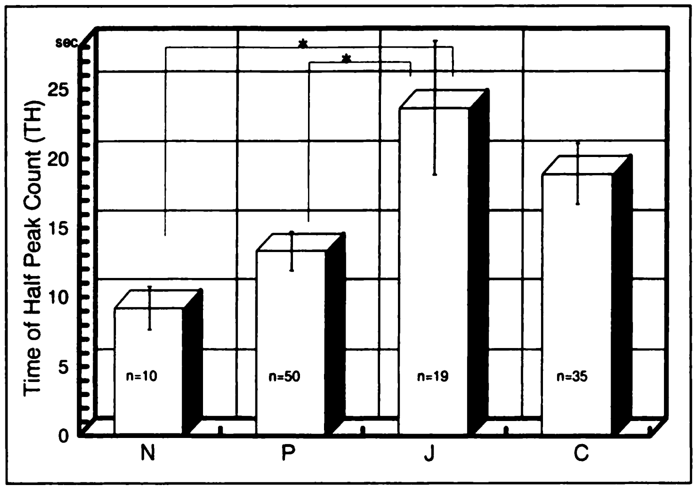

FIGURE 5. Comparison of time of half peak count (TH) between normal subjects and patient groups. *$p < 0.05$. Error bars show 1 s.e.m.

The TH is a parameter which is directly proportional to the persistence of the radionuclide in the subclavian vein and serves as a sensitive index of slow blood flow in the central veins. In Figure 5, an upward trend suggests increasingly sluggish flow through the central veins with the highest values noted for Group J. Interestingly, values of TH register a fall in Group C, owing to availability of collateral pathways. The presence of increased TH per se should not be considered diagnostic of SVC syndrome as has been previously reported (*21*). For diagnostic purposes, it should be considered in combination with other findings such as jugular venous reflux or increased transit time. It may serve as a useful parameter in follow-up studies. The PC ratio also showed an upward trend, similar to TT and TH. This common upward tendency represents the disturbance in blood flow.

Presence of a statistically significant difference of TT and TH between normal subjects and different groups of patients indicates that different hemodynamics are at work in each group. Although, no statistical difference was seen for the PC ratio among the four groups of subjects, we consider the ratio to be potentially useful for follow-up studies. Since none of the indices showed any statistical difference between edematous and nonedematous patients within each group, we may conclude that, hemodynamically, they have similar derangements.

CONCLUSION

Our analysis of the time-activity curves in correlation with the images indicate that:

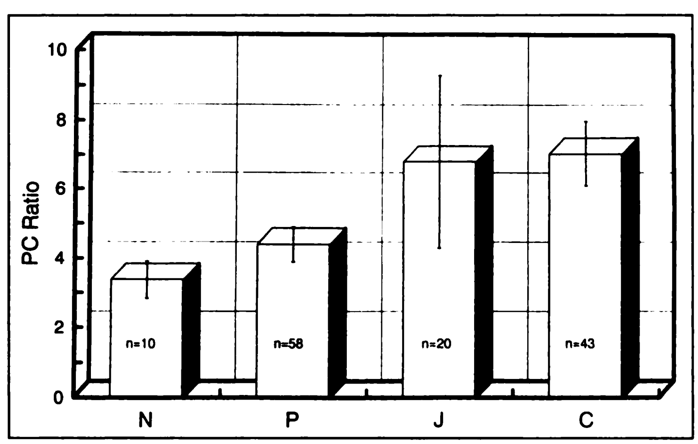

FIGURE 6. Comparison of peak count ratio (PC ratio) between normal subjects and patient groups. Error bars show 1 s.e.m.

1. On radionuclide venography, the presence of jugular venous reflux may serve as an early sign of SVC syndrome, provided other causes of the reflux are ruled out.
2. Prolonged transit time (TT) from subclavian veins to the right atrium is proposed as a useful indicator of slow passage of blood through the central veins.
3. Increased values of time of half-peak count (TH) indicate sluggish blood flow through central veins.
4. The peak count ratio (PC ratio) may be considered a valuable indicator of hemodynamic disturbance in the SVC syndrome.
5. These indices are helpful in detecting hemodynamic changes in patients, irrespective of the presence or absence of clinically manifest edema of the upper half of the body.
6. These indices are potentially useful parameters in follow-up studies of the same patient.

ACKNOWLEDGMENT

We thank Ms. Yuko Ogata for providing technical assistance during the study.

REFERENCES

1. Hunter W. The history of an aneurysm of the aorta with some remarks on aneurysm in general. *Med Observ Inq* 1757;1:323–357.
2. Nieto AF, Doty DB. Superior vena cava obstruction, clinical syndrome, etiology and treatment. *Curr Probl Surg* 1986;10:442–484.
3. Lokich JJ, Goodman R. Superior vena cava syndrome. Clinical management. *JAMA* 1975;231:58–61.
4. Ahman FR. A reassessment of the clinical implications the superior vena cava syndrome. *J Clin Oncol* 1984;2:961–969.
5. Sculier JP, Evans WK, Feld R, et al. Superior vena caval obstruction syndrome in small cell lung cancer. *Cancer* 1986;57:847–851.
6. Yellin A, Rosen A, Riechert N, Lieberman Y. Superior vena cava syndrome. The myth—the facts. *Am Rev Respir Dis* 1990;141:1114–1118.
7. Friedman BH, Lovegrove FTA, Wagner HN. An unusual variant in cerebral circulation studies. *J Nucl Med* 1974;15:363–364.
8. Godfrey K. Comparing the means of several groups. In: Bailar JC III, Mosteller F, ed. *Medical uses of statistics*. Waltham, MA: NEJM Books; 1986;205–234.
9. Van Houtte P, Frühling J. Radionuclide venography in the evaluation of superior vena cava syndrome. *Clin Nucl Med* 1981;6:177–183.
10. Miyamae T. Interpretation of ^{99m}Tc superior vena cavograms and results of studies in 92 patients. *Radiology* 1973;108:339–352.
11. Coltart RS, Wraight EP. The value of radionuclide venography in superior vena cava obstruction. *Clin Radiol* 1985;36:415–418.
12. Muramatsu T, Miyamae T, Doi Y. Collateral pathways observed by radionuclide superior cavography in 70 patients with superior vena caval obstruction. *Clin Nucl Med* 1991;16:332–336.
13. Yedlicka JW, Schultz K, Moncada R, et al. CT findings in superior vena cava obstruction. *Semin Roentgen* 1989;24:84–90.
14. Yeh E, Pohlman GP, Reutz PP, Meade RC. Jugular venous reflux in cerebral radionuclide angiography. *Radiology* 1976;118:730–732.
15. Ogawa TK, So SK, Gerberg E, et al. Jugular—dural sinuses—jugular reflux in dynamic brain flow imaging as a sign of unilateral innominate vein obstruction. *J Nucl Med* 1977;18:39–41.
16. Rao BK, Polcyn RE, Lieberman LM. Influence of respiratory maneuvers on jugular venous reflux. *Clin Nucl Med* 1981;6:23–26.
17. Hayt DB, Perez LA. Cervical venous reflux in dynamic brain scintigraphy. *J Nucl Med* 1976;17:9–12.
18. Blood flow studies. In: Baum S, Vincent NR, Lyons KP, Wu Gurkin SC, eds. *Atlas of nuclear medicine imaging*. New York, NY: Appleton-Century-Crofts; 1981:291–314.
19. Peart RA, Driedger AA. Effect of obstructed mediastinal venous return on dynamic brain blood flow studies: case report. *J Nucl Med* 1975;16:622–625.
20. Vincken W, Roels P, Sonstabo R, et al. Effect of neck position during radionuclide superior cavography. *Clin Nucl Med* 1983;8:424–426.
21. Podoloff DA, Kim EE. Evaluation of sensitivity and specificity of upper extremity radionuclide venography in cancer patients with indwelling central venous catheters. *Clin Nucl Med* 1992;17:457–462.

Iodine-123-MIBG Imaging of Neuroblastoma: Utility of SPECT and Delayed Imaging

Vittoria Rufini, Gregg A. Fisher, Barry L. Shulkin, James C. Sisson and Brahm Shapiro

Division of Nuclear Medicine, Department of Internal Medicine, University of Michigan Medical Center, Ann Arbor, Michigan; and Division of Nuclear Medicine, Sacred Heart Catholic University, Rome, Italy

Possible incremental diagnostic benefits of SPECT and delayed planar imaging with [^{123}I]MIBG in neuroblastoma have not yet been fully established. **Methods:** Whole-body delayed planar [^{123}I]MIBG imaging at 48 hr and SPECT imaging of the chest-abdomen or other suspected sites obtained at 24 hr were compared with routine planar imaging at 24 hr in 83 studies of 29 children with neuroblastoma. The sensitivity for each of the [^{123}I]MIBG imaging methods was calculated on a study-by-study and on a lesion-by-lesion basis. **Results:** Fifty-one planar imaging studies were performed in 20 patients with evidence of disease which was detected in 48 studies by 24-hr imaging (94.1% sensitivity) and in 44 studies by 48-hr imaging (86.3% sensitivity). On a lesion-by-lesion basis, sensitivity was 88.8% for the 24-hr scan, 86.7% for the 48-hr scan and 92.2% for a combination of the two (p = ns). Forty-three SPECT studies were performed in 20 patients with evidence of disease in the field of view of the SPECT camera. Disease was detected in 40 SPECT studies (93% sensitivity), in 38 planar scans at 24 hr (84.4% sensitivity) and in 37 planar scans at 48 hr (86.0% sensitivity). On a lesion-by-lesion basis, sensitivity was 83.6% for the 24-hr planar scan, 86.1% for the 48-hr planar scan, 88.2% for a combination of the two planar scans and 97.9% for SPECT ($p < 0.001$ compared with planar). The anatomic locations of tumors were clearer on SPECT in 15 studies. **Conclusion:** Delayed 48-hr planar scanning may occasionally depict more lesions than 24-hr imaging, but it may also miss lesions with rapid washout. SPECT imaging significantly increases the number of lesions detected and better defines anatomic location of tumors.

Key Words: iodine-123-MIBG; neuroblastoma; planar imaging; delayed imaging; SPECT

J Nucl Med 1996; 37:1464–1468

Metaiodobenzylguanidine (MIBG) labeled with either ^{131}I or ^{123}I has been used for nearly 15 yr in the scintigraphic evaluation of neuroendocrine tumors, particularly pheochromocytomas and neuroblastomas (*1–3*). In patients with neuroblastoma, a sensitivity of 77%–96% and a high specificity (approximately 100%) has been reported for both radiopharmaceuticals (*3–6*). Due to its physical properties (159 keV photon energy, 13-hr half-life and paucity of particulate emission of ^{123}I) and the high activity that can be administered, MIBG labeled with ^{123}I has superior imaging characteristics. These characteristics of [^{123}I]MIBG, and its favorable dosimetry, even in higher administered doses, make its use preferable in children (*7–8*).

Iodine-123-MIBG imaging is most commonly performed at 24 hr after tracer administration. However, the optimal timing for scintigraphy has not been definitively established; a recent report by Paltiel et al. (*9*) points out the improvement of thoraco-abdominal lesion visualization in 48-hr images.

Received Jun. 26, 1995; revision accepted Dec. 27, 1995.

For correspondence or reprints contact: V. Rufini, MD, Division of Nuclear Medicine, Sacred Heart Catholic University, Policlinico Gemelli, Largo A. Gemelli 8, Rome 00168, Italy.